Visualizing perfusion throughout the cardiac cycle using advanced power Doppler acquisition and filtering methods

Abbie Weeks
Department of Biomedical Engineering
Vanderbilt University
Nashville, TN, USA
abbie.e.weeks@vanderbilt.edu

Emelina Vienneau
Department of Biomedical Engineering
Vanderbilt University
Nashville, TN, USA
emelina.p.vienneau@vanderbilt.edu

Brett Byram
Department of Biomedical Engineering
Vanderbilt University
Nashville, TN, USA
brett.c.byram@vanderbilt.edu

***Abstract*— Evaluating blood flow in the liver has clinical implications for functional and oncological assessment. Here, we explore visualization of temporally varying power Doppler signals in the 3 vasculature systems in the liver using coded excitation acquisitions and block-wise SVD filtering that mitigate the limitations of poor SNR, spectral overlap, and shorter ensembles. We acquired 2 seconds of data with matched ECG traces, and then evaluated 100 sample ensembles across the ECG trace to assess optimal cardiac phases for forming images. We show that highest CNR and SNR values are obtained from images formed during diastole.**

Keywords—cardiac cycle, liver, coded excitation, block-wise SVD, ECG

I. Introduction

Evaluating blood flow in well-perfused organs is clinically relevant for cancer treatment and organ function assessment. The liver has three main vasculature systems: hepatic veins, hepatic arteries, and portal veins. Understanding how a tumor has invaded these systems or how each is functioning can potentially guide clinical intervention[1], [2]. However, tissue motion, and poor SNR all reduce data quality, resulting in less informative Doppler outcomes. Many filtering methods use ensembles of a few hundred to several hundred samples to evaluate more temporally stable perfusion[3], [4]. Temproal variations arise from the pulsatility inherent to blood flow and the cardiac cycle[5]–[8]. Here, we explore visualization of temporally varying power Doppler signals in the 3 vasculature systems in the liver using coded excitation acquisitions and block-wise SVD filtering that mitigate the limitations of poor SNR, spectral overlap, and shorter ensembles.

II. Methods

A. Acquisition

We collected 2 seconds of liver data from a healthy volunteer using diverging waves to maximize frame rate and field of-view with a Verasonics Vantage 128 research ultrasound machine [*Verasonics, Kirkland, Washington, USA*]. The data were beamformed using synthetic aperture beamforming. The acquisition sequences employed a 13-bit Barker code excitation sequence to lengthen the transmission pulse and improve SNR. The coded signal was compressed upon receive to recover axial resolution[9], [10]. Figure 1 describes how the coded transmission is created and how the received signal is compressed. Table I details additional acquisition parameters. An ECG signal was collected in conjunction with the power Doppler acquisitions to evaluate variations in blood flow across the cardiac cycle.

TABLE I. Acquisition Parameters

Parameter	Value
Transducer	C5-2
Center Frequency	4.1667 MHz
Angles	-4°:4°, 9 total
Compound PRF	600 Hz
Code Length	13-bit
Acquisition Duration	2 seconds

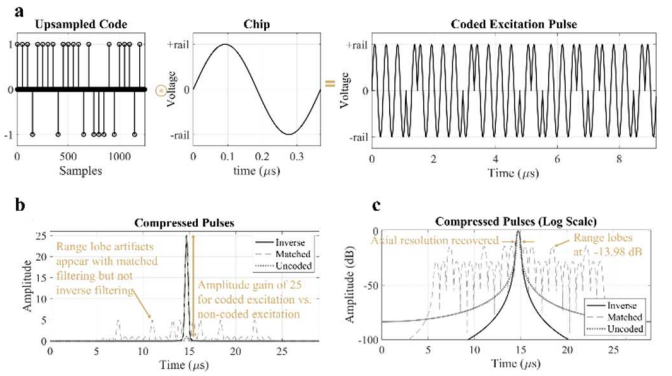

Fig 1. *(a)* Coded excitation lengthens the transmission pulse in order to increase SNR by utilizing Barker codes, binary codes with no zeros in the Fourier Domain. *(b)* Inverse filtering better suppresses range lobe artifacts than matched filtering. *(c)* Axial resolution of image recovered through pulse compression with inverse filtering

B. Filtering

Our goal was to evaluate signal variations across the cardiac cycle. To filter the data, windows of 100 ensemble samples (83 milliseconds), overlapped by 95 samples, were filtered with block-wise SVD [11], [12]. We optimized blood and noise SVD cutoffs for three phases of the cardiac cycle – early diastole, late diastole, and systole – to account for the changes in blood flow and tissue motion throughout the cardiac cycle. The full 2

This work supported by National Science Foundation CAREER award and award IIS-1750994

2022 IEEE International Ultrasonics Symposium (IUS) | 978-1-6654-6657-8/22/$31.00 ©2022 IEEE | DOI: 10.1109/IUS54386.2022.9958230

second ensemble of filtered data was reconstructed with overlapped pixels being averaged.

C. Evaluation

The full 2s filtered ensemble was then divided into packets of 100 samples and overlapped by 95 samples (same as filtering, total of 221 packets) for evaluation. Images were made of each packet and then cineloops made to visually observe changes in blood flow throughout the cardiac cycle. Additionally, ROIs of blood vessels were created and then the power of each ROI in each of the 221 packets was calculated. These power values were plotted through time and compared to the matched ECG signal to observe patterns and correlations. Finally, we tracked CNR and SNR through time for each ROI. We compared these images to those made with 600 sample packets, which corresponds with 1 second and roughly one cardiac cycle. We visually compared the presence of signal across temporal realizations, as well as compared raw power in observed vasculature.

III. Results

Results from a sample case are shown below. Figure 2 shows representative images from each cardiac phase, made from 100 sample ensembles, along with ECG and power Doppler traces for noted ROIs.

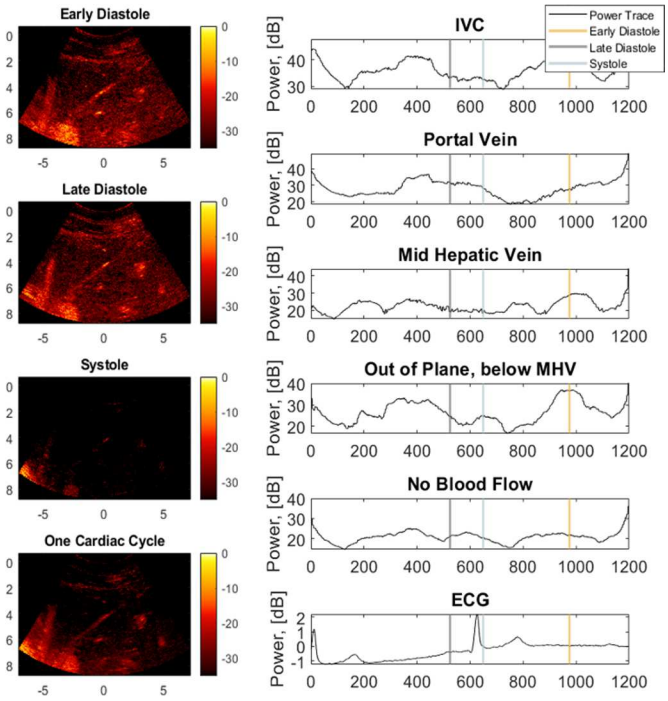

Fig 2. On the left are examples of images taken from each phase of the cardiac cycle. On the right are the corresponding locations in the ECG and power traces where each image came from. Each power trace corresponds to vasculature visible in the images.

Figures 3 and 4 show the CNR and SNR through time as compared with the cardiac cycle.

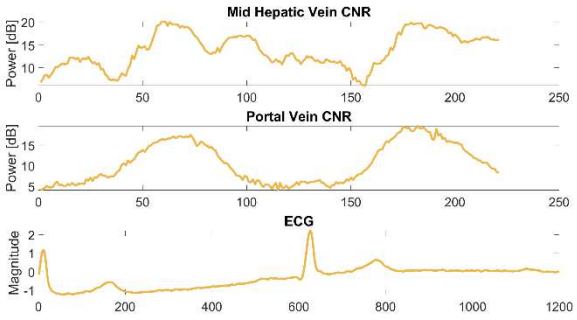

Fig 3. Contrast-to-noise ratio through time compared to ECG.

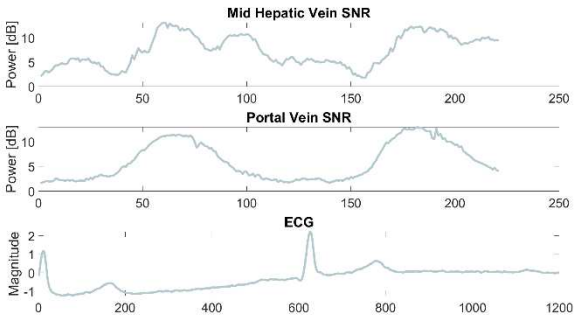

Fig 4. Signal-to-noise ratio through time compared to ECG.

IV. Discussion

As expected, we observed variations in the power Doppler signal throughout the cardiac cycle. The power Doppler traces in Figure 2 have a general 2-cycle structure with peaks that are naturally offset from the ECG trace. Unfortunately, these traces are not compelling enough to determine the type of liver vasculature they are sourced from if blinded to the ROI. However, we can see trends that suggest diastole is the best phase of the cardiac cycle to make images from, and that suggestion is supported further by the CNR and SNR traces through time (Figures 3 and 4). Both CNR and SNR show clear pulsatility with peaks in diastole for both mid hepatic vein and portal vein ROIs.

We found that it was necessary to adapt the SVD thresholds for each segment of the cardiac cycle in order to visualize blood flow in each phase of the cardiac cycle. This is likely due to a combination of slightly increased tissue motion during systole. Going forward, we would like to define a rule for adjusting the SVD thresholds for each phase of the cardiac cycle based on optimized thresholds for one phase of the cardiac cycle (perhaps early diastole, as that seems to be the phase in which we currently make the best images).

This study ultimately focused on higher velocity blood flow in larger blood vessels. We would like to modify our acquisition sequences to employ a faster frame rate to potentially capture slower blood flow, and then perform a similar analysis. While

we observed relatively consistent power and quality metrics in larger vessels, we would expect even more variation in different smaller vasculature of each vascular system in the liver. Ultimately, we could use that information to help determine which vascular systems a tumor has invaded in the liver. That information could then be used to inform interventional decisions in the clinic.

V. Conclusion

In conclusion, we have explored temporal variability of power Doppler signals in the liver. We showed that CNR and SNR metrics display pulsatility that is expected with the pulsatility of the cardiac cycle. While we were not able to clearly identify particular vascular systems through this analysis as anticipated, we did gain intuition for which phases of the cardiac cycle are optimal for making power Doppler images in the liver and we will use that intuition to guide further studies in this area.

Acknowledgment

I would like to thank the Vanderbilt Advanced Computing Center for Research and Education and the Vanderbilt Institute for Surgery and Engineering for their support in this work.

References

[1] E. Leen *et al.*, "Hepatic perfusion changes in patients with liver metastases: comparison with those patients with cirrhosis," *Gut*, vol. 34, pp. 554–557, 1993.

[2] R. Marants *et al.*, "Exploring the Link Between Hepatic Perfusion and Endotoxemia in Hemodialysis," *Kidney Int. Reports*, vol. 6, no. 5, pp. 1336–1345, May 2021, doi: 10.1016/J.EKIR.2021.02.008.

[3] J. Tierney, J. Baker, D. Brown, D. Wilkes, and B. Byram, "Independent Component-Based Spatiotemporal Clutter Filtering for Slow Flow Ultrasound," *IEEE Trans. Med. Imaging*, vol. 39, no. 5, p. 1472, May 2020, doi: 10.1109/TMI.2019.2951465.

[4] K. Ozgun, J. T. Stanton, J. Baker, A. Borgmann, D. Brown, and B. Byram, "Non-contrast power Doppler imaging with multidimensional clutter filtering for assessment of trans-arterial chemoembolization for hepatic malignancy," vol. 11602, no. 15, p. 116020N, Feb. 2021, doi: 10.1117/12.2582109.

[5] N. Zhang, M. B. Nguyen, L. Mertens, D. J. Barron, O. Villemain, and J. Baranger, "Improving coronary ultrafast Doppler angiography using fractional moving blood volume and motion-adaptive ensemble length," *Phys. Med. Biol.*, vol. 67, no. 12, p. 125021, Jun. 2022, doi: 10.1088/1361-6560/AC7430.

[6] Mittal, "Doppler evaluation of hepatic vein flow," *J. Indian Acad. Echocardiogr. Cardiovasc. Imaging*, vol. 2, no. 1, p. 53, 2018, doi: 10.4103/JIAE.JIAE_80_17.

[7] M. H. Scheinfeld, A. Bilali, and M. Koenigsberg, "Understanding the Spectral Doppler Waveform of the Hepatic Veins in Health and Disease1," *https://doi.org/10.1148/rg.297095715*, vol. 29, no. 7, pp. 2081–2098, Nov. 2009, doi: 10.1148/RG.297095715.

[8] D. Aguirre-Reyes, "QUANTIFICATION OF HEPATIC STEATOSIS USING MAGNETIC RESONANCE IMAGING," 2016.

[9] E. Vienneau and B. Byram, "Compound Barker-Coded Excitation for Increased Signal-to-Noise Ratio and Penetration Depth in Transcranial Ultrasound Imaging," *IEEE Int. Ultrason. Symp. IUS*, vol. 2020-September, Sep. 2020, doi: 10.1109/IUS46767.2020.9251650.

[10] E. P. Vienneau and B. C. Byram, "A coded excitation framework for increased signal-to-noise ratio of in vivo ultrasound power Doppler imaging," Feb. 2021, p. 26, doi: 10.1117/12.2582344.

[11] P. Song, A. Manduca, J. D. Trzasko, and S. Chen, "Ultrasound Small Vessel Imaging With Block-Wise Adaptive Local Clutter Filtering," *IEEE Trans. Med. Imaging*, vol. 36, no. 1, pp. 251–262, Jan. 2017, doi: 10.1109/TMI.2016.2605819.

[12] A. Weeks, J. Tierney, and B. Byram, "Block-wise Independent Component Analysis for Slow Flow Non-Contrast Ultrasound Imaging," in *2019 IEEE International Ultrasonics Symposium (IUS)*, Oct. 2019, pp. 2256–2258, doi: 10.1109/ULTSYM.2019.8926293.